*Desalination and Water Treatment*
www.deswater.com
doi: 10.1080/19443994.2015.1070288

57 (2016) 15176–15189
July

Taylor & Francis
Taylor & Francis Group

# Experimental and theoretical studies on the removal of polycarboxy-benzoic acids by adsorption onto polyaniline from aqueous solution

Mohamed Laabd, Abdelhadi El Jaouhari, Hafsa Chafai, Mohammed Bazzaoui, Hassan Kabli, Abdallah Albourine*

*Laboratory of Materials and Environment, Faculty of Sciences, Department of Chemistry, Ibn Zohr University, BP 8106, Agadir 80000, Morocco, emails: mohamed.laabd@edu.uiz.ac.ma (M. Laabd), abdo.eljaouhari@gmail.com (A. El Jaouhari), chafai.hafsa@yahoo.fr (H. Chafai), bazzaoui@fe.up.pt (M. Bazzaoui), kabli.hassan@yahoo.fr (H. Kabli), Tel. +212 528220957; Fax: +212 528220100; email: albourine.abdallah@gmail.com (A. Albourine)*

Received 7 December 2014; Accepted 2 July 2015

ABSTRACT

The adsorption of trimellitic and pyromellitic acids has been performed onto synthesized polyaniline (PANi) by chemical oxidative polymerization. Different parameters that influence the adsorption processes (pH, temperature, ratio solid/liquid, initial concentration, and contact time) had been examined. Adsorption kinetic study indicates a great adjustment with pseudo-second-order kinetic model. The equilibrium data were best fitted by Langmuir isotherm model. The maximum monolayer adsorption capacities are 67.4 and 94.5 mg/g for trimellitic and pyromellitic acids, respectively. Comparison of the adsorption capacities indicates that increasing the number of carboxylic functional groups promotes adsorption on the PANi. Thermodynamic parameters ($\Delta H^\circ$, $\Delta S^\circ$, and $\Delta G^\circ$) indicate that the adsorption is spontaneous and endothermic in nature. The calculations of chemical quantum parameters were performed for optimized molecular structures using the AM1 and MINDO semi-empirical methods. The theoretical data were well correlated with the experimental results.

*Keywords:* Adsorption; Polyaniline; Polycarboxy-benzoic acids; Quantum chemical calculations

## 1. Introduction

The problem of wastewater contamination by various pollutants, such as humic acids, dyes, pesticides, heavy metals, etc., has become a major concern for a number of years. The toxicity of these pollutants presents significant risks to either of the ecosystem or human health, which requires the effective use of treatment processes capable of extracting harmful elements [1,2].

Humic substances constitute a major fraction of natural organic matter (NOM); they exist in natural water with high concentrations, giving the water a yellow-brown color. Humic and fulvic acids have a strong complexing power vis-à-vis metal ions [3–5].

NOM exist in aquatic ecosystems with concentrations ranging of organic carbon between 0.5 and 100 mg/L. It undergoes biological, chemical, and photochemical transformations and generally produces carboxylic acids of low molecular weight, such as benzene polycarboxylic acids and polyhydroxy benzene polycarboxylic acids. These acids behave as

*Corresponding author.

surfactants due to their functional groups [6–9]. The removal of such compounds in industrial wastewater is important because they are widely produced and used as intermediate reactants in the fabrication of resins, plasticizers, dyes, printing inks, and polymers; also, the elimination of this compound from natural water in purification stations can be of interest because they constitute model pollutants originating from biodegradation of biomass [10]. In order to remove these pollutants, several separation techniques can be used to treat wastewater or polluted water: chemical precipitation, ion exchange, biosorption, adsorption [11–13]. In this work, we chose the adsorption as an effective decontamination technique.

The influence of chemical compounds molecular structure on their reactivity is of great interest in various fields of chemistry. For this, it is necessary to use quantum chemistry calculations to study the electronic structure and energy to interpret experimental results. The adsorption of the organic compounds is the yield of the molecular structure of the adsorbate and the adsorbent; therefore, it is useful to confirm these characteristics theoretically.

The objective of this study was the elimination of two humic acid derivatives (Fig. 1): Trimellitic (1,2,3-benzene tricarboxylic acid) and pyromellitic (1,2,4,5-benzene tetracarboxylic acid) acids by adsorption, both compounds being known as toxic herbicides. For this, we have made a systematic study of the effect of different parameters that influence the adsorption phenomenon on the polyaniline (PANi): pH, temperature, contact time, adsorbent dose, and adsorbate initial concentration.

To complete the experimental study, we performed theoretical calculations using two semi-empirical methods of quantum chemistry: Austin Model 1 (AM1) and Modified Neglect of Differential Overlap (MNDO) methods implemented in the MOPAC 2012 software. We can also deduce the effect of structural and energetic parameters of studied systems on their chemical reactivity.

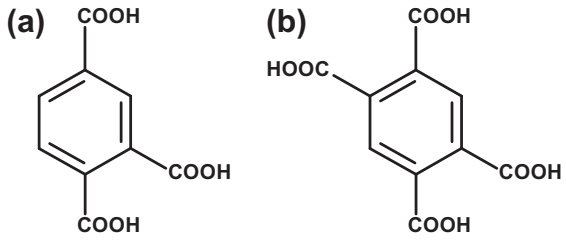


Fig. 1. Chemical structure of adsorbates: (a) trimellitic acid and (b) pyromellitic acid.

## 2. Materials and methods

### 2.1. Reagents and solutions

Aniline ($C_6H_7N$), the commercial product used, is distilled before its polymerization. The oxidizing agent is sodium persulfate hexahydrate ($Na_2S_2O_8{\cdot}6H_2O$).

The solutions of the two trimellitic ($C_9H_6O_6$) and pyromellitic ($C_{10}H_6O_8$) acids with respective molar masses of 210.14 and 254.16 g/mol are prepared from solid trimellitic and pyromellitic acids dissolved in distilled water.

### 2.2. Preparation of adsorbent

The chemical synthesis of the PANi is achieved by using the oxidant ($Na_2O_8S_2{\cdot}6H_2O$) in hydrochloric acid (1 M), with a molar ratio of monomer/oxidant = 1/2 (Fig. 2). The mixture was stirred magnetically for two hours at room temperature. The obtained product (dark green) was then washed with distilled water to remove traces of monomer and oligomers, then with ethanol to remove oxidant traces. Finally, the polymer was oven-dried at 65°C for 3 h [14,15].

### 2.3. Method of analysis

The samples, collected after adsorption, are filtered through filters of 0.45 μm porosity. The concentrations were measured using a UV/visible spectrometer (JENWAY 6405). The absorption maximum wavelengths of trimellitic and pyromellitic acids are 210 and 215 nm, respectively. The adsorption efficiency and adsorbed quantity are calculated by the following Eqs. (1) and (2):

$$\text{The adsorbed quantity}: Q_e = (C_0 - C_e)V/m \ \left(\text{mg/g}\right) \quad (1)$$

$$\text{The adsorption efficiency}: R(\%) = (C_0 - C_e)100/C_0 \quad (2)$$

$C_0$ and $C_e$ are, respectively, the initial and equilibrium concentrations (mg/L). $V/m$: volume/support mass (L/g).

### 2.4. Quantum chemical calculations

The theoretical approach carried out aims to explain the experimentally observed phenomena during adsorption of trimellitic and pyromellitic acids on the PANi. It would also contribute to the establishment of an adsorption mechanism.

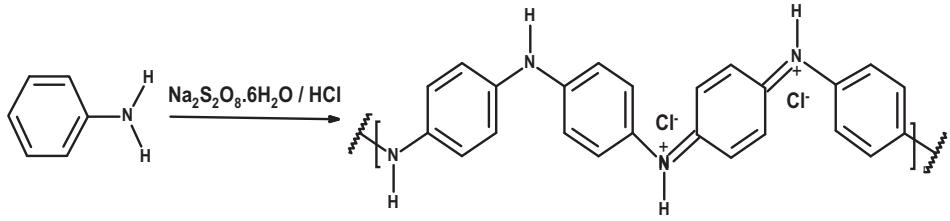


Fig. 2. Oxidative polymerization reaction of aniline.

Quantum chemical parameters and geometric structures of the studied acids have been optimized using the AM1 and MNDO methods implemented in the MOPAC 2012 software and the Davidon Fletcher-Powell algorithm with the "PRECISE" option [16–18]. The semi-empirical methods (AM1 and MNDO) were chosen because they are well adapted to the calculation of the quantum parameters of medium or large molecular systems [19].

The application of frontier molecular orbital theory is an effective way to interpret the reactivity of molecules based on information of the energies and coefficients of their molecular orbital [20–23]. In fact, the reactivity of a system is based on the interaction between its frontier molecular orbitals to know the highest occupied molecular orbital (HOMO) and lowest unoccupied molecular orbital (LUMO). In this regard, the stability of the formed systems (adsorbent-adsorbate) depends essentially on the gap energy $\Delta E_{gap} = E_{HOMO} - E_{LUMO}$. The interaction energy increases gradually as the energy difference between the frontiers molecular orbital decreases.

## 3. Results and discussion

Elimination of trimellitic and pyromellitic acids by adsorption on the PANi is achieved by evaluating the effect of various parameters on the retention capacity, such as pH, temperature, the ratio: mass of the support/volume of the solute, kinetics, and adsorption isotherms.

### 3.1. Effect of adsorbent dose

To study the effect of the ratio: weight of the PANi/volume of the solute, the initial concentration of the adsorbate is set at 10 mg/L in a solution of a volume of 150 mL. The mass of the PANi is varied between 0.01 and 0.25 g for a contact time of 60 min. Adsorption is based on the transfer of matter from the liquid to the solid state. The adsorbent mass has a substantial effect on the adsorption performance. Examination of Fig. 3 shows an increase in the adsorption efficiency with the mass of the PANi. This can be explained by the increase of available adsorption sites of trimellitic and pyromellitic acids. The optimal ratios ($m/V$) are 0.67 g/L for trimellitic acid and 0.20 g/L for pyromellitic acid. In the remainder of this work, we use optimal ($m/V$) ratios for each system.

### 3.2. Kinetic study

The adsorption kinetics allows describing the reaction rates and determines the contact time set to achieve saturation of the support. Thus, we followed trimellitic and pyromellitic acids adsorption kinetics to an initial concentration of 10 mg/L, with ratios (mass of support)/(volume of the solute) for trimellitic and pyromellitic acids of 0.67 and 0.20 g/L, respectively.

To determine the optimal contact time and the adsorbed quantities at equilibrium, an adsorption study is performed by varying the contact time between 5 and 360 min (Fig. 4).

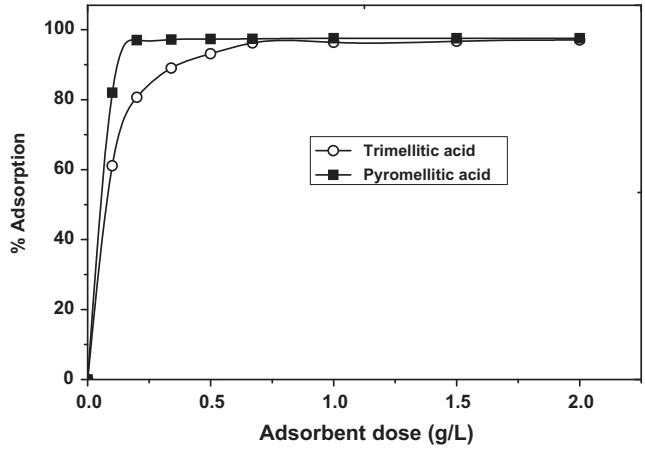


Fig. 3. Effect of adsorbent dose on the adsorption of trimellitic and pyromellitic acids on the PANi. Experimental conditions: $C_0$ = 10 mg/L; $t$ = 60 min; $T$ = 25°C at pH 6.

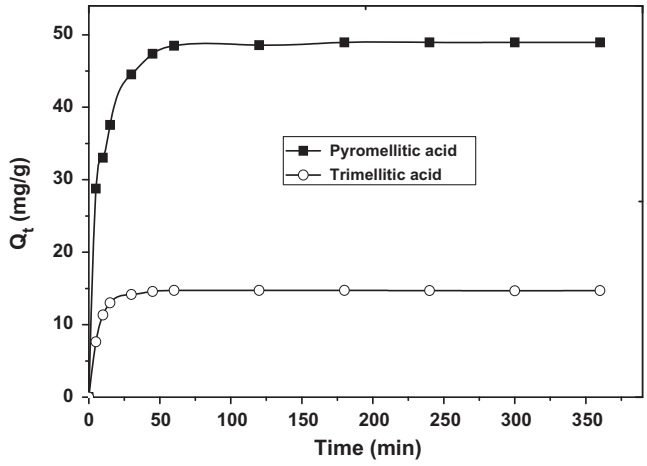


Fig. 4. Effect of contact time on the adsorption of trimellitic and pyromellitic acids on the PANi. Experimental conditions: $C_0$ = 10 mg/L; $R_{TMA}$ = 0.67 g/L; $R_{PMA}$ = 0.20 g/L; $T$ = 25°C at pH 6.

The results obtained show that the adsorption of pollutants is performed in two stages:

(1) A rapid stage in which an increase in the retention capacity of trimellitic and pyromellitic acids by PANi observed during the first minutes of solid/liquid contact. This increase is the result of the occupation of free active sites. In fact, the transfer of the adsorbate molecules to the outer surface of the adsorbent is important as long as the solution concentration is large.
(2) A second stage which shows saturation plateau after contact of 60 min.

We also note that $Q_e$ (trimellitic acid) < $Q_e$ (pyromellitic acid). This can be justified by the large number of carboxylic groups substituted on the aromatic ring in the case of pyromellitic acid.

Several kinetic models, namely pseudo-first-order, pseudo-second-order, and intraparticle diffusion models have been used for their validity with the experimental adsorption results for the trimellitic and pyromellitic acids on the PANi.

Kinetic pseudo-first-order model with linear expression (Fig. 5(a)) is expressed by the Eq. (3) [24]:

$$\ln(Q_e - Q_t) = \ln Q_e - K_1 t \quad (3)$$

Kinetic pseudo-second-order model with linear expression (Fig. 5(b)) is given by the following Eq. (4) [25]:

$$t/Q_t = 1/K_2 Q_t^2 + t/Q_e \quad (4)$$

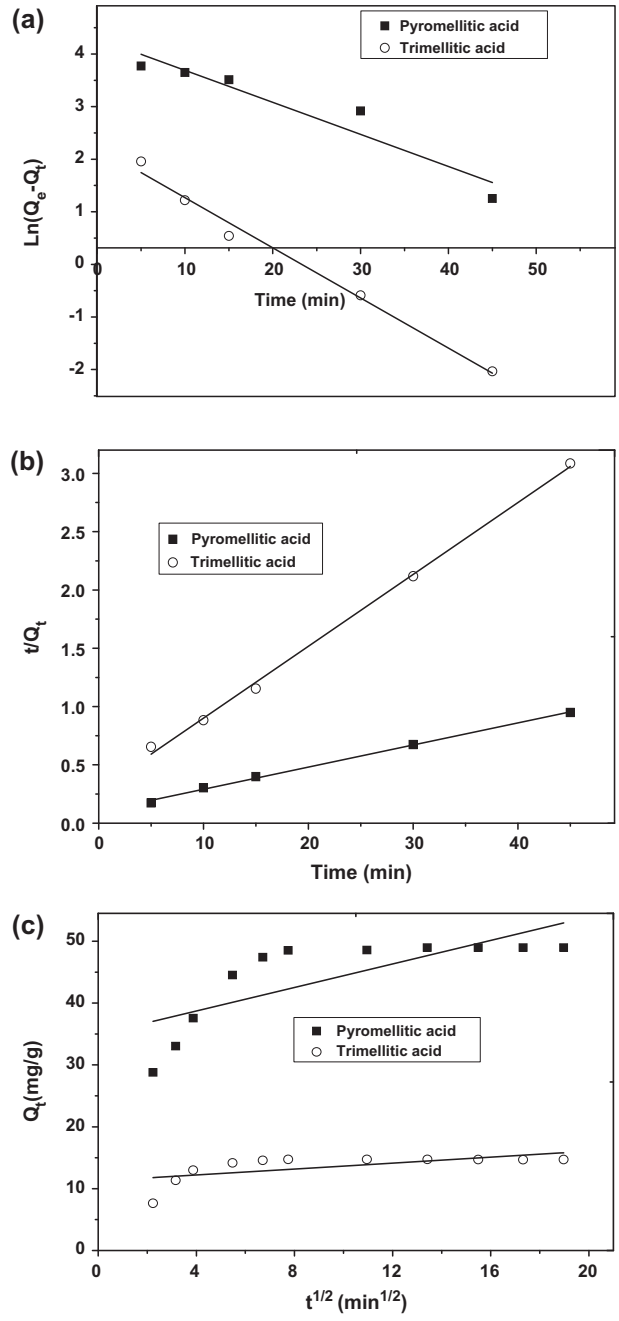


Fig. 5. The pseudo-first-order (a), pseudo-second-order (b), and intraparticle diffusion (c) kinetic plot for adsorption of trimellitic and pyromellitic acids on the PANi.

Intraparticle diffusion model with linear expression (Fig. 5(c)) is given by Weber Morris [26] (Eq. (5)):

$$Q_t = K_p t^{1/2} + C \quad (5)$$

where $K_1$, $K_2$, and $K_p$ is the constant of pseudo-first-order ($min^{-1}$), pseudo-second-order, (g/mg min) and intraparticle diffusion (mg/g $min^{1/2}$), respectively.

The values of different kinetic parameters are summarized in Table 1. The values of correlation coefficients ($R^2$) for the second-order kinetic model were greater than 0.997 for trimellitic and pyromellitic acids, indicating the applicability of the second-order kinetic model to describe the adsorption process of studied adsorbates on the PANi. Besides, the experimental adsorbed quantities ($Q_e$ (trimellitic acid) = 14.7 mg/g and $Q_e$ (pyromellitic acid) = 48.5 m/g) are close to the theoretical values obtained by the pseudo-second-order model ($Q_e$ (trimellitic acid) = 16.39 mg/g and $Q_e$ (pyromellitic acid) = 52.63 mg/g). Based on the values of the kinetic constants $K_2$, the retention rate of the two adsorbates is quite fast.

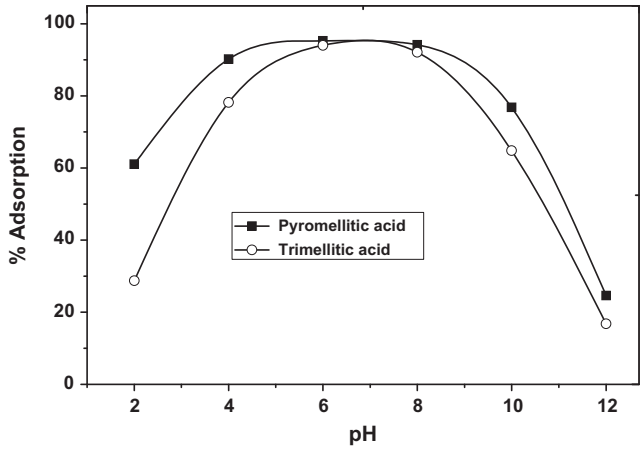


Fig. 6. Effect of pH on the adsorption of trimellitic and pyromellitic acids on the PANi. Experimental conditions: $C_0$ = 10 mg/L; $R_{TMA}$ = 0.67 g/L; $R_{PMA}$ = 0.2 g/L; $t$ = 60 min at $T$ = 25°C.

### 3.3. Effect of initial pH

The investigation of the influence of solution pH on the adsorption efficiency of trimellitic and pyromellitic acids on PANi is carried out in a pH range of 2–12. It is recalled that the pH of the solutions of the two studied pollutants with the same initial concentration 10 mg/L was adjusted by NaOH or HCl (1 M). The mass of the adsorbent is 0.1 g for trimellitic acid and 0.03 g for pyromellitic acid in a solution volume of 150 mL.

The experimental results in Fig. 6 highlight three distinct areas:

(1) pH < 5, where there is a low capacity of PANi to fix adsorbates. This can be justified by the partial deprotonation of the carboxylic functions (Fig. 7). The functional groups which are not deprotonated are not adsorbed by the PANi, thereby reducing the rate of adsorption. The partial deprotonation occurs by the following reactions [27,28].

(2) 5 ≤ pH ≤ 9, wherein the adsorption efficiency reaches a value of 94%, all the carboxylic functions of the two pollutants are deprotonated (Fig. 7).

(3) pH > 9: adsorption efficiency decreases for the two adsorbates. This is due to the relatively significant competition between conjugate bases of trimellitic and pyromellitic acids and excessive $OH^-$ ions on one hand. On the other hand, it is due to the transformation of the emeraldine salt (conductive form) to the emeraldine base (insulating form); in highly basic conditions [29].

### 3.4. Effect of temperature

For examining the temperature influence on the adsorption of the trimellitic and pyromellitic acids onto PANi, we vary the temperature of the solution

Table 1
Kinetic parameters for the adsorption of trimellitic and pyromellitic acids on the PANi

| Kinetic models | Constants | Trimellitic acid | Pyromellitic acid |
|---|---|---|---|
| Kinetic pseudo-first-order | $R^2$ | 0.988 | 0.994 |
| | $Q_e$ (mg/g) | 9.235 | 31.125 |
| | $K_1$ ($min^{-1}$) | 0.095 | 0.072 |
| Kinetic pseudo-second-order | $R^2$ | 0.998 | 0.997 |
| | $Q_e$ (mg/g) | 16.39 | 52.63 |
| | $K_2$(g/mg min) | 0.0131 | 0.0036 |
| Intraparticle diffusion | $R^2$ | 0.414 | 0.589 |
| | $k_p$ (mg/g $min^{1/2}$) | 0.24 | 0.949 |
| | $C$ | 11.24 | 34.92 |

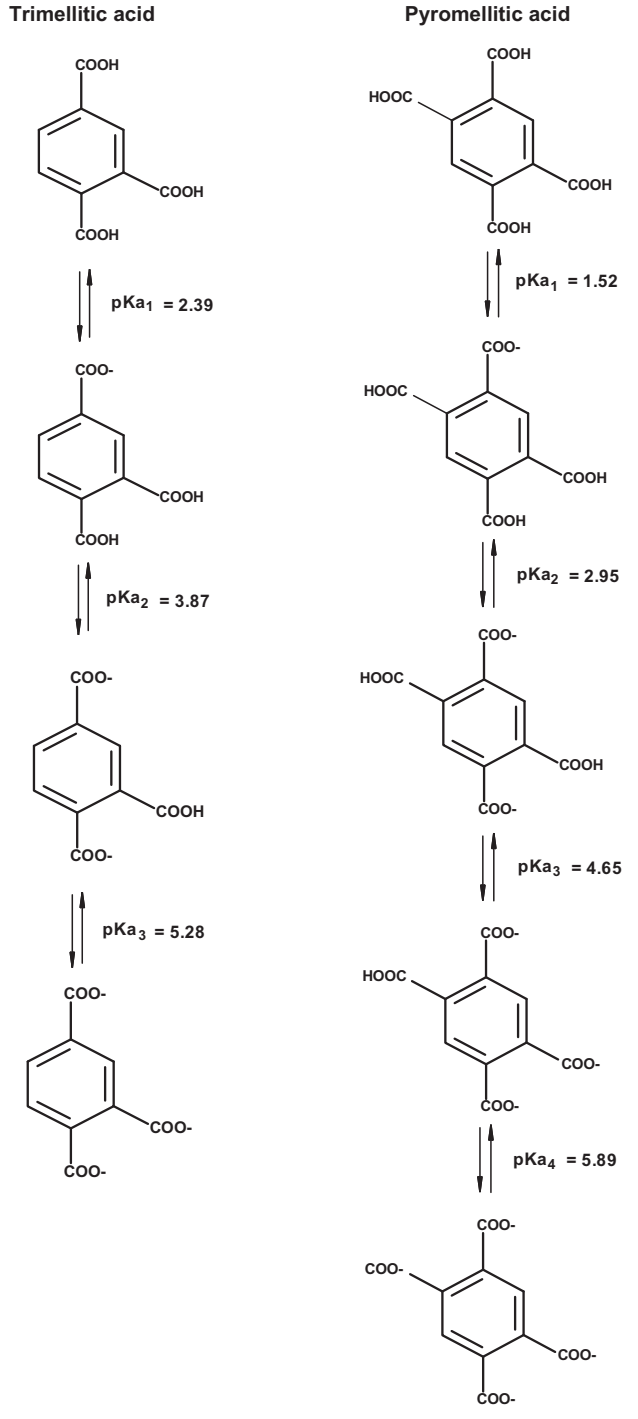


Fig. 7. Deprotonation reactions and p$K_a$ values of trimellitic and pyromellitic acids.

by means of a thermostatic bath keeping the other parameters constant. The obtained results are shown in Fig. 8. Adsorbed amounts are practically constant when the thermal agitation increases in the temperature range studied.

### 3.5. Adsorption isotherms

The adsorption isotherms were determined by varying the initial concentrations from 10 to 200 mg/L with a support dose of 0.67 g/L for trimellitic acid and 0.2 g/L for the pyromellitic acid in room temperature for a contact time of 60 min. Fig. 9 shows the variation of the adsorbed amount based on the initial concentration of the two adsorbates studied. According to the results, we note that the adsorbed quantities of the two adsorbates increase with the initial concentration. This may be due to the increase of the amount of adsorbate molecules in the vicinity of the support which increases the probability of an adsorbent–adsorbate encounter and also increases the attractive forces between the positively charged active sites of the support and the negatively charged carboxylic functional groups of the adsorbates. In addition, the intergranular diffusion of the adsorbate increases with initial concentration. The variation of the adsorbed amount depending on the initial concentration ends by a saturation stage reflecting the almost full utilization of the energy active sites.

The linear functions of models of adsorption isotherms are expressed by the following Eqs. (6)–(9):

The Langmuir isotherm model [30,31] expressed as Eq. (6):

$$C_e/Q_e = 1/K_L Q_m + C_e/Q_m \quad (6)$$

where $K_L$ is the constant of Langmuir; $C_e$ is residual concentration in the solution at adsorption equilibrium (mg/L); $Q_e$ and $Q_m$ are equilibrium and maximum adsorbed quantities (mg/g).

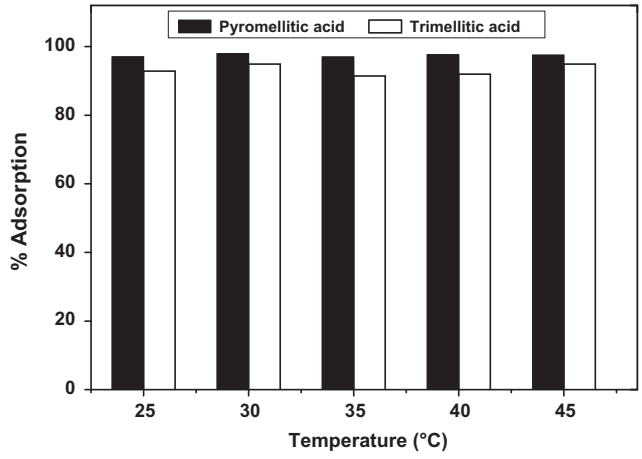


Fig. 8. Effect of temperature on the adsorption of trimellitic and pyromellitic acids onto PANi. Experimental conditions: $C_0$ = 10 mg/L; $R_{TMA}$ = 0.67 g/L; $R_{PMA}$ = 0.2 g/L; $t$ = 60 min at pH 6.

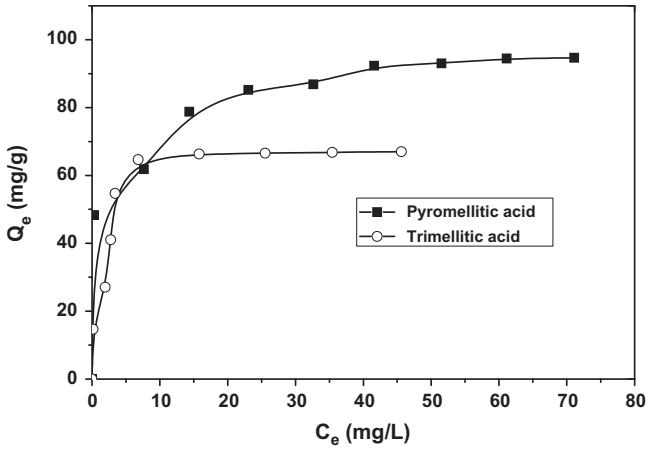


Fig. 9. Effect of initial concentration on the adsorption of trimellitic and pyromellitic acids on the PANi. Experimental conditions: $R_{TMA}$ = 0.67 g/L; $R_{PMA}$ = 0.20 g/L; $t$ = 60 min; $T$ = 25°C at pH 6.

$R_L$ (dimensionless) is the separation factor, with $R_L = 1/(1 + K_L C_0)$

The value of $R_L$ indicates the type of isotherm to be irreversible ($R_L = 0$), favorable ($0 < R_L < 1$), linear ($R_L = 1$), or unfavorable ($R_L > 1$).

The Freundlich isotherm equation [32] is given as:

$$\ln Q_e = \ln K_f + 1/n_f \ln C_e \quad (7)$$

where $K_f$ is the Freundlich constant represents the relative adsorption capacity of the adsorbent and $n_f$ represents the degree of dependence of adsorption on the equilibrium concentration of adsorbates.

The linear expression of Temkin isotherm model [33] is shown below:

$$Q_e = B \ln K_T + B \ln C_e \quad (8)$$

where $K_T$ and $B$ are constants of Temkin.

The Generalized isotherm [33] is an empirical model and can be linearized in logarithmic form as follows:

$$\ln(Q_m/Q_e - 1) = \ln K - N_b \ln C_e \quad (9)$$

where $K$ and $N_b$ are constants of saturation and coordination bond, respectively.

The linear plots of the models of Langmuir, Freundlich, Temkin, and Generalized are presented by Fig. 10.

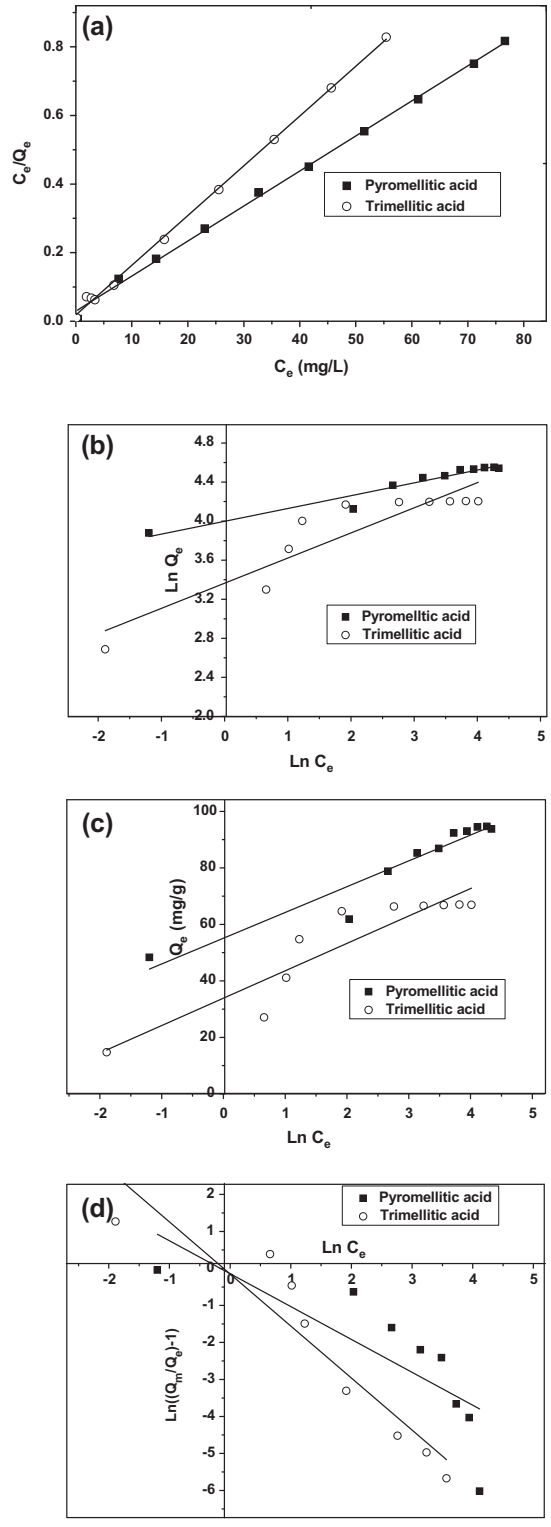


Fig. 10. The Langmuir (a), Freundlich (b), Temkin (c), and Generalized (d) adsorption isotherms of trimellitic and pyromellitic acids on the PANi.

Table 2
Langmuir, Freundlich, Temkin, and Generalized isotherm model parameters and correlation coefficients for adsorption of trimellitic and pyromellitic acids on the PANi

| Isotherms | Constants | Trimellitic acid | Pyromellitic acid |
|---|---|---|---|
| Langmuir | $R^2$ | 0.999 | 0.998 |
| | $K_L$ | 0.933 | 0.357 |
| | $Q_m$ (mg/g) | 71. 43 | 100 |
| | $R_L$ | 0.005–0.096 | 0.027–0.218 |
| Freundlich | $R^2$ | 0.574 | 0.941 |
| | $K_f$ | 37.554 | 54.707 |
| | $n_f$ | 6.802 | 7.751 |
| Temkin | $R^2$ | 0.634 | 0.919 |
| | $K_T$ | 229.9 | 450.3 |
| | $B$ | 7.135 | 9.054 |
| Generalized | $R^2$ | 0.764 | 0.853 |
| | $K$ | 1.053 | 0.854 |
| | $n_b$ | 0.729 | 0.567 |

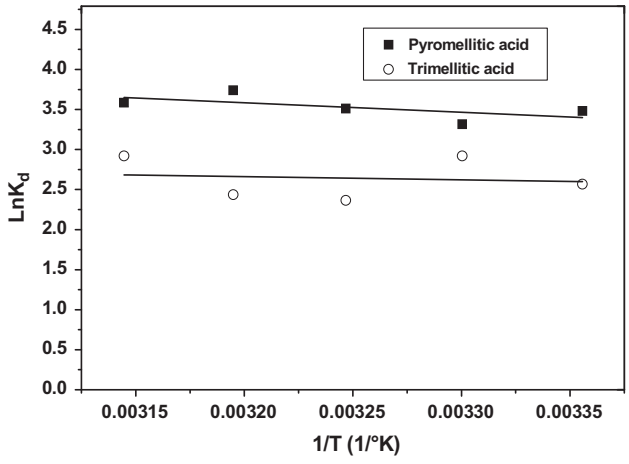


Fig. 11. Arrhenius plots for adsorption of trimellitic and pyromellitic acids on the PANi. Experimental conditions: $C_0$ = 10 mg/L; $R_{ATM}$ = 0.67 g/L; $R_{APM}$ = 0.2 g/L; $t$ = 60 min at pH 6.

Correlation coefficients ($R^2$), the adsorbed quantities, and constants of the four models of adsorption isotherms are summarized in Table 2.

Based on the results of Table 2, the correlation coefficients are close to 1, and as a result, the adsorption of two adsorbates on the PANi seems to follow the Langmuir model. This indicates that the adsorbent surface is energetically uniform and there are no interactions among adsorbed molecules. Also, each molecule occupies a specific site until the formation of a monolayer [31]. Thus, we can see that the maximum monolayer adsorption quantities obtained by the Langmuir isotherm ($Q_{m,Théo}$ (Trimellitic acid) = 71.43 mg/g and $Q_{m,Théo}$ (Pyromellitic acid) = 100 mg/g), are very close to those obtained experimentally ($Q_{m,Exp}$ (Trimellitic acid) = 67.4 mg/g and $Q_{m,Exp}$ (Pyromellitic acid) = 94.5 mg/g). Also the value of the separation factor $R_L$ is between 0 and 1 (validity range) for the two adsorbates. This strengthens the validity of the Langmuir model.

### 3.6. Adsorption thermodynamics

Thermodynamic parameters ($K_d$, $\Delta H^\circ$, $\Delta S^\circ$, and $\Delta G^\circ$) related to the adsorption reaction of trimellitic and pyromellitic acids at equilibrium are represented by the Eqs. (10)–(12) (Fig. 11) [34,35].

$$\ln K_d = \Delta S^\circ/R - \Delta H^\circ/TR \quad (10)$$

where $R$ (8.314 J/mol K) is the perfect gas constant, and $T$ is the absolute solution temperature (Kelvin).

Table 3
Thermodynamic parameters for adsorption of trimellitic and pyromellitic acids on the PANi

| | | | $\Delta G^\circ$ (kJ/mol) | | | | |
|---|---|---|---|---|---|---|---|
| Adsorbates | $\Delta H^\circ$ (kJ/mol) | $\Delta S^\circ$ (J/mol K) | 298 K | 303 K | 308 K | 313 K | 318 K |
| Trimellitic acid | 3.28 | 32.6 | −6.33 | −7.36 | −6.06 | −6.34 | −7.72 |
| Pyromellitic acid | 9.89 | 61.4 | −8.63 | −8.36 | −8.99 | −9.73 | −9.48 |

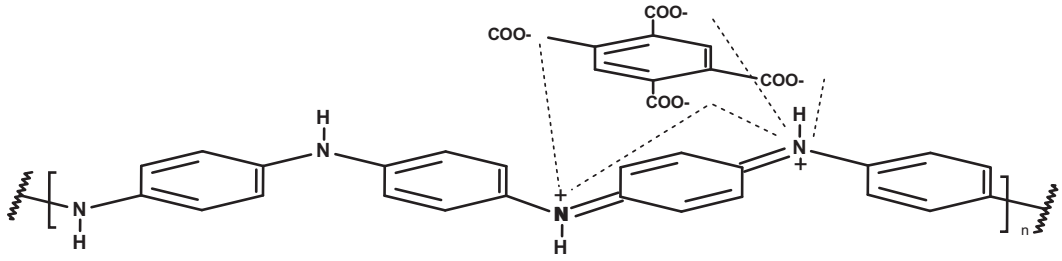


Pyromellitic acid/PANi Horizontal adsorption

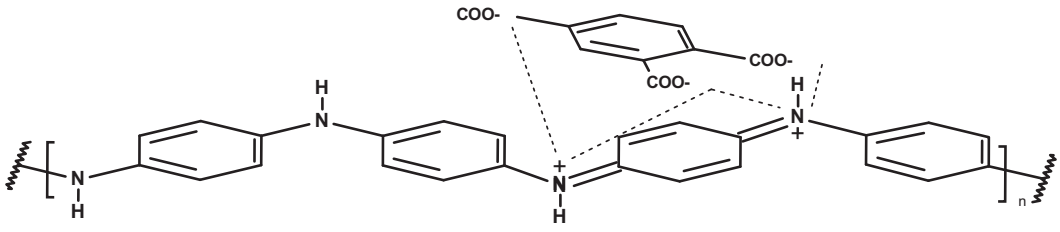


Trimellitic acid/PANi Horizontal adsorption

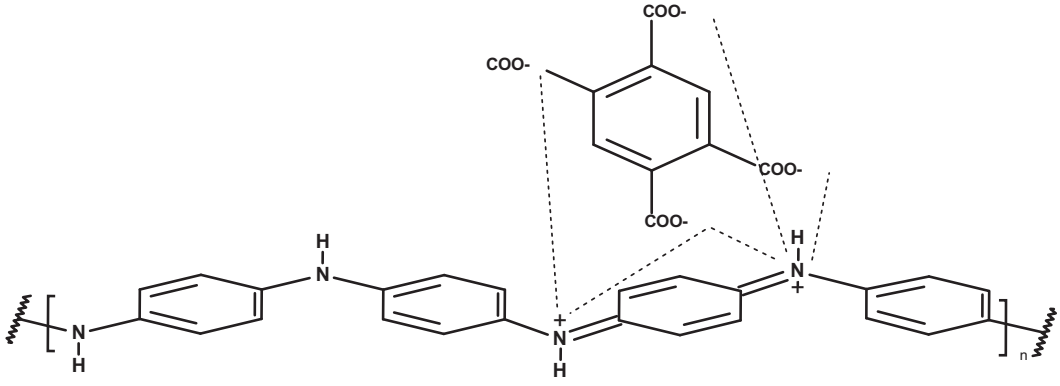


Pyromellitic acid/PANi Vertical adsorption

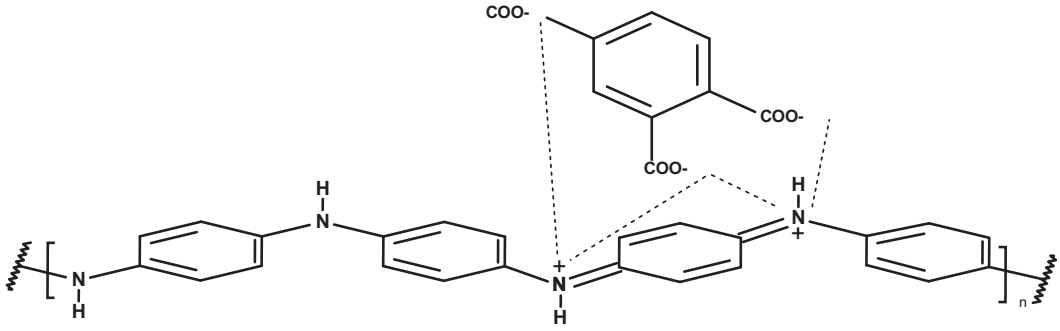


Trimellitic acid/PANi Vertical adsorption

---------- Electrostatic interactions between adsorbate and adsorbent

Fig. 12. Proposed mechanism for the adsorption of trimellitic and pyromellitic acids on the PANi.

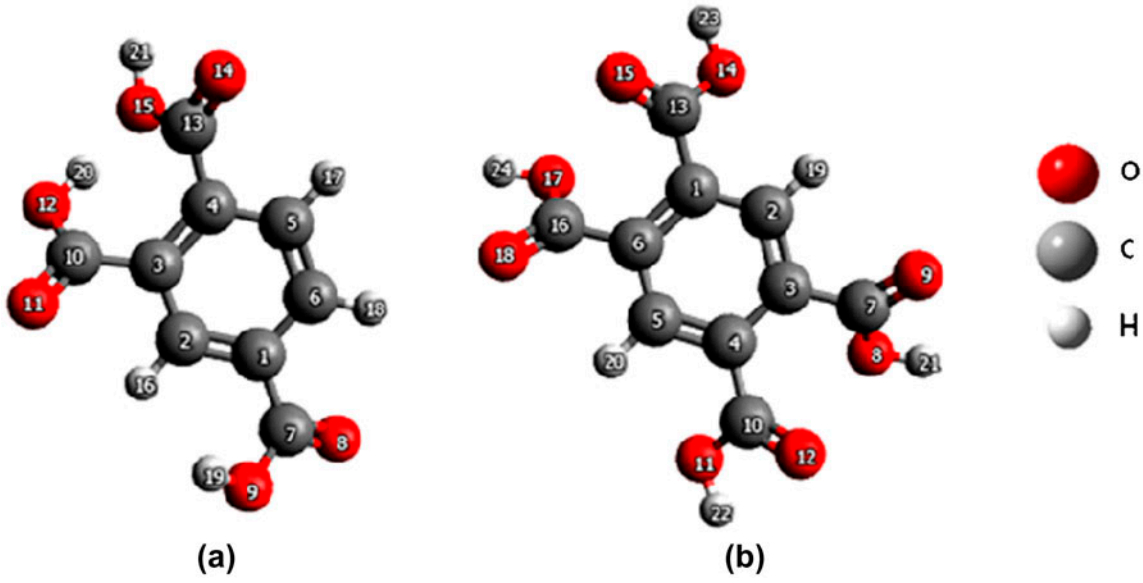


Fig. 13. Optimized molecular structures of (a) trimellitic and (b) pyromellitic acids.

Table 4
Net atomic charges of trimellitic and pyromellitic acids calculated by the AM1 and MNDO methods.

| | | AM1 | | MNDO | |
|---|---|---|---|---|---|
| Number | Atom | Trimellitic acid | Pyromellitic acid | Trimellitic acid | Pyromellitic acid |
| 1 | C | −0.128 | −0.038 | −0.131 | −0.021 |
| 2 | C | −0.075 | −0.054 | 0.025 | 0.015 |
| 3 | C | −0.102 | −0.038 | −0.105 | −0.023 |
| 4 | C | −0.051 | −0.038 | −0.010 | −0.021 |
| 5 | C | −0.089 | −0.054 | −0.030 | 0.015 |
| 6 | C | −0.062 | −0.038 | 0.009 | −0.023 |
| 7 | C | 0.336 | 0.351 | 0.370 | 0.377 |
| 8 | O | −0.280 | −0.298 | −0.294 | −0.295 |
| 9 | O | −0.276 | −0.333 | −0.275 | −0.331 |
| 10 | C | 0.342 | 0.351 | 0.364 | 0.378 |
| 11 | O | −0.287 | −0.307 | −0.289 | −0.291 |
| 12 | O | −0.266 | −0.332 | −0.272 | −0.338 |
| 13 | C | 0.343 | 0.351 | 0.375 | 0.378 |
| 14 | O | −0.326 | −0.307 | −0.329 | −0.291 |
| 15 | O | −0.328 | −0.332 | −0.303 | −0.338 |
| 16 | C | – | 0.351 | – | 0.377 |
| 17 | O | – | −0.298 | – | −0.295 |
| 18 | O | – | −0.333 | – | −0.331 |

The distribution constant $K_d$ is calculated using the equation : $K_d = C_r V / m C_e$ (11)

$C_r$ and $C_e$ are, respectively, the retained and equilibrium concentrations of the adsorbate.

The standard free enthalpy is calculated by the equation : $\Delta G^\circ = -RT \ln K_d$ (12)

From the results of Table 3, the positive values of the standard enthalpy $\Delta H^\circ$ show the endothermic nature

Table 5
The quantum chemical parameters (frontier molecular orbitals) of the trimellitic and pyromellitic acids calculated by the AM1 and MNDO methods

| Methods | Acids | $E_{HOMO}$ (eV) | $E_{LUMO}$ (eV) | $\Delta E_{LUMO-HOMO}$ (eV) |
|---|---|---|---|---|
| AM1 | Trimellitic | −11.358 | −1.875 | 9.483 |
| | Pyromellitic | −11.768 | −2.404 | 9.364 |
| MNDO | Trimellitic | −10.838 | −1.497 | 9.341 |
| | Pyromellitic | −10.736 | −1.480 | 9.256 |

for both studied acids. The values of standard free enthalpy at different temperatures are negative ($\Delta G^\circ < 0$) demonstrating a spontaneous adsorption phenomenon. We also note that $\Delta G^\circ$ (pyromellitic acid) < $\Delta G^\circ$ (trimellitic acid) at different temperatures. This means that the adsorption of the pyromellitic acid is more favorable than that of trimellitic acid. The low positive values of adsorption entropy $\Delta S^\circ$ of trimellitic and pyromellitic acids indicate randomness in the solid–liquid interface [36,37]. The values of $\Delta G^\circ$ range between −20 and 0 kJ/mol. This suggests that the adsorption mechanism of trimellitic and pyromellitic acids on PANi is a physisorption type [38]. Fig. 12 illustrates the proposed mechanism for this physical adsorption. The intermolecular interactions between the polycarboxy-benzoic acids and the PANi are electrostatic attractions between polar functional groups of the adsorbate (carboxylate functions) and the nitrogen heteroatom of the PANi. Two adsorption modes are possible:

(1) Horizontal adsorption when the lateral interactions between molecules are low,
(2) Vertical adsorption when the adsorption competition between the adsorbate and the solvent is insignificant [39].

## 4. Theoretical study

In this study, quantum chemical calculations were conducted by the AM1 and MNDO methods by optimized geometries of the studied compound. This is to support experimental data and to investigate the relationship between molecular structure of the polycarboxy-benzoic acids and their adsorption efficiency. Fig. 13 represents the optimized structures of trimellitic and pyromellitic acids.

The distribution of the atomic charge is used as an important index of the chemical reactivity of the molecules. The electric charge of the molecules is responsible for the electrostatic interactions between the adsorbate and the adsorbent. The analysis of the electronic data in Table 4 shows a very high charge density on the oxygen atoms and electron deficiency in carbon atoms in both studied molecules for AM1 and MNDO methods. This explains that the adsorption on the surface of the PANi (positively charged) occurs through the oxygen atoms. The electronic density of the pyromellitic acid is greater compared to that of trimellitic acid. This indicates that the increased number of carboxylic functional groups results in an increase of the total charge density of the molecule, therefore increasing the adsorption efficiency.

Calculations of net charges of trimellitic acid show negative charges of $O_{14}$ and $O_{15}$ larger than that of the other oxygen atoms. The corresponding carboxylic group would be more favorable to adsorption compared with other carboxylic groups. In the contrary, pyromellitic acid (symmetric molecule) shows similar carboxylic groups. This was taken into consideration in the adsorption mechanism proposed above (Fig. 12).

Table 5 shows the calculated energetic parameters for both studied benzene polycarboxylic acids by the AM1 and MNDO methods. From the results of Table 5, we note that the energy difference ($\Delta E_{HOMO-LUMO}$) between the HOMO and LUMO decreases from the trimellitic acid to the pyromellitic acid. This leads to the transfer of the electrons which becomes easier with a decrease in the energy gap ($\Delta E_{HOMO-LUMO}$); thus, the adsorption efficiency increases. These results also indicate that the charge transfer of the adsorbate to the adsorbent has taken place during the adsorption on the surface of the PANi.

Based on data of quantum parameters (HOMO, LUMO, and $\Delta E_{HOMO-LUMO}$), chemical reactivity of the pyromellitic acid is greater than that of trimellitic acid. So we can expect better adsorption performance of pyromellitic acid. This is confirmed experimentally by the retained quantities of the adsorbates: $Q_{max}$ (Pyromellitic acid) > $Q_{max}$ (trimellitic acid).

## 5. Conclusions

The study of the adsorption of trimellitic and pyromellitic acids in aqueous solution on the PANi in static mode reveals the following conclusions:

(1) The retained amount of the adsorbates increases with the adsorbent dose and generates an increase in active sites involved in the adsorption process;
(2) For a pH < 5: The adsorption is weak; this is due to the small amount of deprotonated carboxylic groups in accordance with p$K_a$ values;
(3) For the pH range comprised between 5 and 9: The adsorption is maximized, as a result carboxylic groups are completely deprotonated;
(4) As for pH > 9: There is a decrease in the adsorption efficiency. The excess of $OH^-$ ions enter in direct competition with the conjugate bases (trimellitates and pyromellitates);
(5) The influence of temperature on the adsorption of pollutants on PANi is practically negligible;
(6) The kinetic models plots show that the adsorption kinetics respond better to the pseudo-second-order model;
(7) The thermodynamic study shows that the adsorption processes are endothermic and spontaneous in nature;
(8) The study of the retention mechanism of the two adsorbates shows a better fit to the model of Langmuir;
(9) The adsorption is promoted by the increase number of functional carboxylic groups involved in the adsorption process of the studied compounds ($Q_m$ (trimellitic acid) < $Q_m$ (pyromellitic acid));
(10) The data obtained from quantum chemical calculations (electronic charge density and frontier molecular orbital) using the AM1 and MNDO methods showed better agreement with the experimental results.

## List of Symbols

AM1 — Austin Model 1
$C_0$ — initial concentrations (mg/L)
$C_e$ — equilibrium concentrations (mg/L)
$\Delta E$ — energy gap (eV)
$\Delta G^\circ$ — standard free enthalpy of adsorption (KJ/mol)
HOMO — highest occupied molecular orbital
$\Delta H^\circ$ — standard enthalpy of adsorption (KJ/mol)
$K$ — constant of saturation
$K_1$ — rate constant for pseudo-first-order kinetic model ($min^{-1}$)
$K_2$ — rate constant of pseudo-second-order kinetic model (g/mg min)
$K_d$ — distribution constant (L/g)
$K_f$ — Freundlich constant represents the relative adsorption capacity of the adsorbent (mg/g)
$K_L$ — constant of Langmuir related with the energy of the adsorption (L/mg)
$K_p$ — rate constant of intraparticle diffusion kinetic model (mg/g $min^{1/2}$)
$K_T$ and $B$ — constants of Temkin
LUMO — lowest unoccupied molecular orbital
MNDO — modified neglect of differential overlap
$N_b$ — constant of coordination bond
$n_f$ — constant of Freundlich represents the degree of dependence of adsorption on the equilibrium concentration of adsorbates
NOM — natural organic matter
PANi — polyaniline
Pyromellitic acid — 1,2,4,5-benzene tetracarboxylic acid
$Q_e$ — amount adsorbed at equilibrium (mg/g)
$Q_m$ — maximum adsorbed quantity (mg/g)
$Q_t$ — amount adsorbed at any time $t$ (mg/g)
$R$ (8.314 J/mol K) — perfect gas constant
$R_L$ — separation factor
$R_{PMA}$ — ratio ($m/V$) for pyromellitic acid (g/L)
$R_{TMA}$ — ratio ($m/V$) for trimellitic acid (g/L)
$\Delta S^\circ$ — entropy of adsorption (J/mol K)
Trimellitic acid — 1,2,3-benzene tricarboxylic acid

## References

[1] G.W. Aherne, J. English, V. Marks, The role of immunoassay in the analysis of microcontaminants in water samples, Ecotoxicol. Environ. Saf. 9 (1985) 79–83.
[2] A. Begum, S. HariKrishna, I. Khan, Analysis of heavy metals in water, sediments and fish samples of Madivala Lakes of Bangalore, Karnataka, Int. J. ChemTech Res. 1 (2009) 245–249.
[3] A. Begum, S. HariKrishna, Bioaccumulation of trace metals by aquatic plants, Int. J. ChemTech Res. 2 (2010) 250–254.
[4] J.F. McCarthy, B.D. Jimenez, Interactions between polycyclic aromatic hydrocarbons and dissolved humic material: Binding and dissociation, Environ. Sci. Technol. 19 (1985) 1072–1076.
[5] C.T. Chiou, D.E. Kile, T.J. Brinton, R.L. Malcolm, J.A. Leenheer, P. MacCarthy, A comparison of water solubility enhancements of organic solutes by aquatic humic materials and commercial humic acids, Environ. Sci. Technol. 21 (1987) 1231–1234.
[6] F.H. Frimmel, Characterization of natural organic matter as major constituents in aquatic systems, J. Contam. Hydrol. 35 (1998) 201–216.
[7] F.M. Benoit, R. Helleur, M. Malaiyandi, S. Ramaswamy, D. Williams, Soil fulvic acid degradation by ozone in aqueous medium, Ozone Sci. Eng. 15 (1993) 19–38.

[8] S. Bertilsson, L.J. Tranvik, Photochemical transformation of dissolved organic matter in lakes, Limnol. Oceanogr. 45 (2000) 753–762.
[9] A. Jonsson, L. Ström, J. Åberg, Composition and variations in the occurrence of dissolved free simple organic compounds of an unproductive lake ecosystem in northern Sweden, Biogeochemistry 82 (2007) 153–163.
[10] A. Assabbane, Y. Ait Ichou, H. Tahiri, C. Guillard, J.M. Herrmann, Photocatalytic degradation of polycarboxylic benzoic acids in UV-irradiated aqueous suspensions of titania. Identification of intermediates and reaction pathway of the photomineralization of trimellitic acid (1,2,4-benzene tricarboxylic acid), Appl. Catal., B Environ. 24 (2000) 71–87.
[11] N. Kleefstra, S.T. Houweling, S.J.L. Bakker, S. Verhoeven, R.O. Gans, B. Meyboom-de Jong, H.J.G. Bilo, Chromium treatment has no effect in patients with type 2 diabetes in a western population: A randomized, double-blind, placebo-controlled trial, Diabetes Care 30 (2007) 1092–1096.
[12] A. Terbouche, C. Ait Ramdane-Terbouche, D. Hauchard, S. Djebbar, Evaluation of adsorption capacities of humic acids extracted from Algerian soil on polyaniline for application to remove pollutants such as Cd(II), Zn(II) and Ni(II) and characterization with cavity microelectrode, J. Environ. Sci. 23 (2011) 1095–1103.
[13] M.J. González-Muñoz, M. Amparo Rodríguez, S.A. Luque, J. Ramón Álvarez, Recovery of heavy metals from metal industry waste waters by chemical precipitation and nanofiltration, Desalination 200 (2006) 742–744.
[14] A. Pron, F. Genoud, C. Menardo, M. Nechtschein, The effect of the oxidation conditions on the chemical polymerization of polyaniline, Synth. Met. 24 (1988) 193–201.
[15] Y. Cao, A. Andreatta, A.J. Heeger, P. Smith, Influence of chemical polymerization conditions on the properties of polyaniline, Polymer 30 (1989) 2305–2311.
[16] W.C. Davidon, Variance algorithm for minimization, Comput. J. 10 (1968) 406–410.
[17] M.J.S. Dewar, W. Thiel, Ground states of molecules. 38. The MNDO method. Approximations and parameters, J. Am. Chem. Soc. 99 (1977) 4899–4907.
[18] M.J.S. Dewar, E.G. Zoebisch, E.F. Healy, J.J.P. Stewart, Development and use of quantum mechanical molecular models. 76. AM1: A new general purpose quantum mechanical molecular model, J. Am. Chem. Soc. 107 (1985) 3902–3909.
[19] M.I. Bernal-Uruchurtu, M.T.C. Martins-Costa, C. Millot, M.F. Ruiz-López, Improving description of hydrogen bonds at the semiempirical level: Water-water interactions as test case, J. Comput. Chem. 21 (2000) 572–581.
[20] N. Dennis, A.R. Katritzky, H. Wild, 1,3-Dipolar character of six-membered aromatic rings. Part XXVII. Photochemically induced valence bond tautomerism and dimerisation of 3-oxido-1-phenylpyridinium J. Chem. Soc., Perkin Trans. 1(21) (1976) 2338–2343, doi: 10.1039/P19760002338.
[21] M. Harju, P.L. Andersson, P. Haglund, M. Tysklind, Multivariate physicochemical characterisation and quantitative structure–property relationship modelling of polybrominated diphenyl ethers, Chemosphere 47 (2002) 375–384.
[22] J.W. Chen, T. Harner, P. Yang, X. Quan, S. Chen, K.W. Schramm, A. Kettrup, Quantitative predictive models for octanol–air partition coefficients of polybrominated diphenyl ethers at different temperatures, Chemosphere 51 (2003) 577–584.
[23] A. Kitti, M. Harju, M. Tysklind, B. van Bavel, Multivariate characterization of polycyclic aromatic hydrocarbons using semi-empirical molecule orbital calculations and physical data, Chemosphere 50 (2003) 627–637.
[24] Y. Bulut, H. Aydın, A kinetics and thermodynamics study of methylene blue adsorption on wheat shells, Desalination 194 (2006) 259–267.
[25] V. Vadivelan, K.V. Kumar, Equilibrium, kinetics, mechanism and process design for the sorption of methylene blue onto rice husk, J. Colloid Interface Sci. 286 (2005) 90–100.
[26] T.S. Anirudhan, K.P. Shubha, C. Raji, Immobilization of heavy metals from aqueous solutions using polyacrylamide grafted hydrous tin(IV) oxide gel having carboxylate functional groups, Water Res. 35 (2001) 300–310.
[27] A. Assabbane, S. Qourzal, M. Tamimi, A. Albourine, Y. Ait Ichou, M. Petit-Ramel, Complexes binaires et ternaires du mercure(II) avec quelques acides benzène polycarboxyliques (Binary and ternary complexes of mercury (II) with some benzene polycarboxylic acids), Phys. Chem. News 29 (2006) 81–88.
[28] C.R. Evanko, D.A. Dzombak, Influence of structural features on sorption of nom-analogue organic acids to goethite, Environ. Sci. Technol. 32 (1998) 2846–2855.
[29] A.G. MacDiarmid, "Synthetic Metals": A novel role for organic polymers (Nobel Lecture) Copyright (c) the Nobel Foundation, , We thank the Nobel Foundation Stockholm, for permission to print this lecture Angew. Chem. Int. Ed. in English 40 (2001) (2001) 2581–2590.
[30] C.K. Jain, Adsorption of zinc onto bed sediments of the River Ganga: Adsorption models and kinetics, Hydrol. Sci. J. 46 (2001) 419–434.
[31] M. Muthukrishnan, B.K. Guha, Heavy metal separation by using surface modified nanofiltration membrane, Desalination 200 (2006) 351–353.
[32] M.E. Argun, S. Dursun, C. Ozdemir, M. Karatas, Heavy metal adsorption by modified oak sawdust: Thermodynamics and kinetics, J. Hazard. Mater. 141 (2007) 77–85.
[33] M. Hosseini, S.F.L. Mertens, M. Ghorbani, M.R. Arshadi, Asymmetrical Schiff bases as inhibitors of mild steel corrosion in sulphuric acid media, Mater. Chem. Phys. 78 (2003) 800–808.
[34] M.S. Sajab, C.H. Chia, S. Zakaria, S.M. Jani, M.K. Ayob, K.L. Chee, P.S. Khiew, W.S. Chiu, Citric acid modified kenaf core fibres for removal of methylene blue from aqueous solution, Bioresource Technol. 102 (2011) 7237–7243.
[35] A. Bentouami, M.S. Ouali, Cadmium removal from aqueous solutions by hydroxy-8 quinoleine intercalated bentonite, J. Colloid Interface Sci. 293 (2006) 270–277.
[36] M. Alkan, Ö. Demirbaş, S. Çelikçapa, M. Doğan, Sorption of acid red 57 from aqueous solution onto sepiolite, J. Hazard. Mater. 116 (2004) 135–145.

[37] M. Doğan, M. Alkan, Ü. Çakir, Electrokinetic properties of perlite, J. Colloid Interface Sci. 192 (1997) 114–118.
[38] M. Auta, B.H. Hameed, Modified mesoporous clay adsorbent for adsorption isotherm and kinetics of methylene blue, Chem. Eng. J. 198–199 (2012) 219–227.
[39] C.H. Giles, D. Smith, A general treatment and classification of the solute adsorption isotherm: I. Theoretical, J. Colloid Interface Sci., 47 (1974) 755–765.